ICAS 2021 SHANG HAI
International Council of the Aeronautical Sciences
32nd Congress of the International Council of the Aeronautical Sciences
September 6-10, 2021
Pudong Shangri-La, Shanghai, China

A Benchmark Method for Predicting Oblique Shock Structure

Aiming Shi[1], Earl H. Dowell[2]

[1]Department of Fluid Mechanics, NPU-Duke Topic Group for Aerodynamics and Aeroelasticity, Northwestern Polytechnical University, 127 West Youyi Road, Xi'an, P.R.China 710072 (Email: sam@nwpu.edu.cn);
[2]Department of Mechanical Engineering and Materials Science, NPU-Duke Topic Group for Aerodynamics and Aeroelasticity (TGAA), Duke University, Box 90300 Hudson Hall, Durham, NC USA 27708-0300.

Abstract

The spatial scheme method and adaptive mesh technique are chosen directly to determine the accuracy of the shock capture. Judging the correctness of one scheme by one dimensional Burgers equation is probably not enough for some real situation. A benchmark model for checking shock capturing accuracy is built from the oblique shock strength rule. Combining with the adaptive mesh technique, the simulation results of different discretization schemes are distinguished effectively by the benchmark model. It will provide one single-form of discretization schemes verification.

Keywords: Computational fluid dynamics, Shock waves, Model buildings.

Nomenclature

ROE	=	Roe Flux Differencing Scheme
HLLC	=	Harten - Lax - Van Leer Contact wave solver
HLLE	=	Harten-Lax-van Leer-Einfeldt
AUSM	=	Advection Upstream Split Method
AUSMDV	=	An improved AUSM aiming at removing numerical dissipation of the Van Leer-type flux vector splittings on a contact discontinuity
AUSMPW	=	AUSM by pressure-based weight functions
AUSM+UP	=	Advection upstream splitting method requiring for first order upwind schemes
AUSM+UP2	=	Advection upstream splitting method requiring for 2nd order upwind schemes
CUSP	=	Convective upstream split pressure scheme
VANLEER	=	Van Leer Flux Splitting Scheme
STEGER	=	Steger-Warming scheme

1. Introduction

A high precision in the description of shock structure is one of the goals for Computational Fluid Dynamics (CFD) modelling. In a CFD simulation process, the spatial scheme method and adaptive mesh technique chosen directly determine the accuracy of the shock capture. In order to meet the computational requirements of different flow fields, a variety of spatial discretization schemes have been developed, so how to verify the advantages and disadvantages of a discretization scheme has always been an important problem in computational fluid dynamics. Generally, one dimensional Burgers equation is used to verify the correctness of the scheme. It is probably not enough, however, for some certain real cases. One dimension can basically not representative of higher dimensions. It may bring some potential errors when the scheme is dealing with two- or three-dimensional problem. In fact, the two-dimensional structure is the most general and typical type of CFD computation, because one-dimensional structure is covered by two-dimensional structure and three-dimensional

usually can simplify into two. The oblique shock as the most typical shock structure in two-dimension problem is very significant for determining the accuracy of the shock capture.
Recently, an intensity distribution rule for oblique shock wave has been developed. A benchmark model for checking shock capture accuracy is built from the oblique shock strength rule. In this paper, several frequently used schemes to solve the Euler equations are studied by using the shock strength rule. The tested discretization methods will include the ROE, HLLC, AUSM, AUSM+UP, AUSM+UP2 and CUSP schemes. Adaptive mesh techniques are applied so that all schemes achieve their limits in predicting the shock discontinuities.
In section 2, the shock strength rule is described, and explained the intensity-symmetry property of an oblique shock. Some numerical calculation settings are represented in section 3. Discussions for CFD result are given in section 4.

2. Shock strength rule

Generally, the static pressure ratio before and after the shock wave is used to measure the shock intensity. Due to the static pressure ratio is a monotonic increased function of the normal Mach number, the normal Mach number can be used as the characteristic quantity of oblique shock intensity. For the normal Mach number before the shock wave,

$$M_{n1} = M_1 \cdot \sin\beta \tag{1}$$

where M_1 is the Mach number before the shock. β is the shock wave angle. M_{n1} is the normal Mach number. According to the oblique shock relations,

$$\tan\theta = \frac{\sin 2\beta\left(M_{n1}^2 - 1\right)}{M_{n1}^2(\gamma + \cos 2\beta) + 2(1 - \cos 2\beta)} \tag{2}$$

equation 3 can be obtained by equation 1 and 2. So equation 3 may be defined as the oblique shock strength relation. The oblique shock strength distribution is diagrammed in figure 1.

$$M_{n1}^2 = 1 + \frac{(\gamma+1)\sin\theta}{\sin(2\beta - \theta) - \gamma\sin\theta} \tag{3}$$

Where θ is the deflection angle. γ is the specific ratio.

2.1 Equal shock strength expressed by shock angle

In equation 3, the shock strength is only related to the shock angle β when the deflection angle θ is fixed. The normal Mach number M_{n1} become the smallest as $2\beta-\theta$ equal to 90 degrees, which is just the control equation of the minimum shock strength line in figure 1. Mathematically, equation 3 also shows the symmetrical properties for shock intensity relative to the minimum shock strength value. As deflected angle θ is constant, one normal Mach number can obtain two reasonable shock angles by symmetry of the sine function. Therefore, one can obtain two shock structure of the same strength if the shock angles β_1, β_2 satisfy the following conditions:

$$\beta_1 + \beta_2 = \frac{\pi}{2} + \theta \tag{4}$$

Equation 4 is the control equation of the same shock strength expressed by shock wave angle. It means that one can easily design two shock wave structure giving the same impact in flow field when the deflection angle is fixed. Combining the oblique shock relations, the related intensity-symmetry Mach numbers can be obtained.
The intensity-symmetry property can be easily understood combining the figure 1. At the both side of minimum shock strength line, points representing different shock intensities always appear in pairs and the shock angle of pairs is always one above the line and one below, just like looking in a mirror.

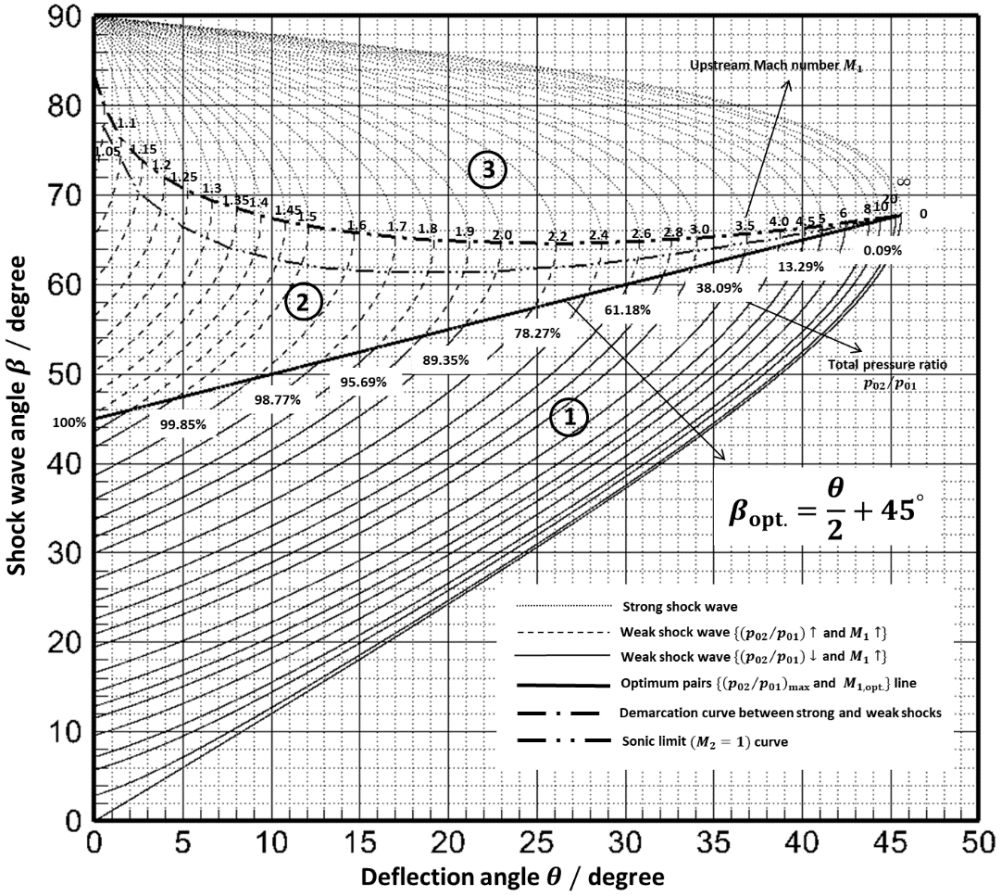

Figure 1 – Minimum shock strength line on the classical θ-β-M diagram. For a fixed deflection angle, Mach number cross the line is the condition to obtain the minimum shock strength. The two equal shock strength values are symmetrical regarding the minimum shock strength.

2.2. Equal shock strength expressed by total pressure loss

Using the total pressure ratio formula of thermodynamic entropy increase, the formula of total pressure loss ratio can be obtained as follows:

$$\frac{\Delta p_0}{p_{01}} = 1 - \left\{ \frac{\left[\frac{(\gamma+1)M_{n1}^2}{2+(\gamma-1)M_{n1}^2} \right]^{\gamma}}{1+\frac{2\gamma}{\gamma+1}\left(M_{n1}^2-1\right)} \right\}^{\frac{1}{\gamma-1}} \tag{5}$$

Take M_{n1} as the independent variable, and take the derivative of equation 5, equation 6 can be obtained:

$$\frac{\Delta p_0}{p_{01}}'\left(M_{n1}\right) = 2M_{n1}\cdot\frac{\gamma}{\gamma-1}\left\{ \frac{\left[\frac{(\gamma+1)M_{n1}^2}{2+(\gamma-1)M_{n1}^2} \right]^{\gamma}}{1+\frac{2\gamma}{\gamma+1}\left(M_{n1}^2-1\right)} \right\}^{\frac{1}{\gamma-1}} \cdot \frac{2(\gamma-1)\left(M_{n1}^2-1\right)^2}{\left[\gamma+1+2\gamma\left(M_{n1}^2-1\right)\right]\left[2M_{n1}^2+(\gamma-1)M_{n1}^4\right]} \tag{6}$$

Since γ=1.4, $M_{n1}\geqslant 1$, equation 6 is greater than 0, equation 5 is a monotonic increment function with M_{n1} as its independent variable. In other words, the shock strength can be represented by the total pressure loss ratio. When the total pressure loss ratio increase, the strength of oblique shock increases correspondingly.

As shown in figure 2, because the minimum total pressure loss rate line appears in the middle of the weak solution region of the oblique shock wave, under the condition of a fixed wedge angle of the wedge, the same total pressure loss rate will result in two groups of different shock front Mach number and shock deflection angle in some intervals on both sides of the line of the minimum total pressure loss rate. One group is large Mach number and small shock angle; another group of small Mach number, large shock Angle. This phenomenon is called a linear symmetric double solution of equal total pressure loss rate with respect to the minimum total pressure loss rate.

The examples of wedge angle of 10 degrees and 20 degrees are provided in figure 2, which describing the phenomenon of double-solutions regarding the line for ratio minimum loss of total pressure. For example, when the deflection angle is 10 degrees and the loss of total pressure is 2.28 percent, there are two solutions, one is the smaller Mach number M_1=1.423 and the larger shock angle β=67.44° in red box, the other one is the larger Mach number M_1=2.438 and the small shock angle β=32.56° in blue box.

Figure 3 shows the corresponding transformation relationship between the shock front Mach number and the shock deflection angle during the generation of the double solution of the normal Mn1. Two more equivalent shock intensity points are provided ($1^{\#}$ and $1^{\#\#}$, $3^{\#}$and $3^{\#\#}$) in figure 3. It should be noting that the shock wave deflection angle of the double solution value of Mn1 in the figure on the right is completely symmetric with respect to the shock wave angle of 50° of the minimum total pressure loss rate line. According to the synthesis of M_{n1} from M_1 and sinβ in the figure on the left, the mechanism by which both (small M_1, big β) and (big M_1, small β) can produce the same M_{n1} may be explained as two steady state solutions of physical compression (Mach number) and spatial compression (shock Angle).

Therefore, a benchmark case can be constructed for predicting the same shock strength by using the two intensity-symmetry Mach numbers or loss of total pressure.

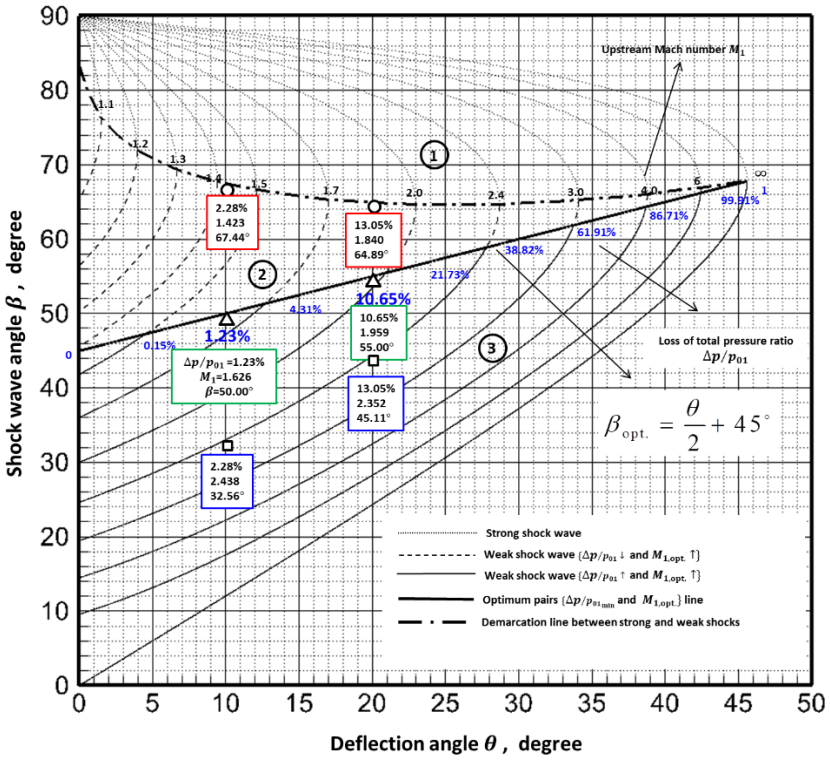

Figure 2 – Double-solutions regarding the line for ratio minimum loss of total pressure in the θ-β-M diagram.

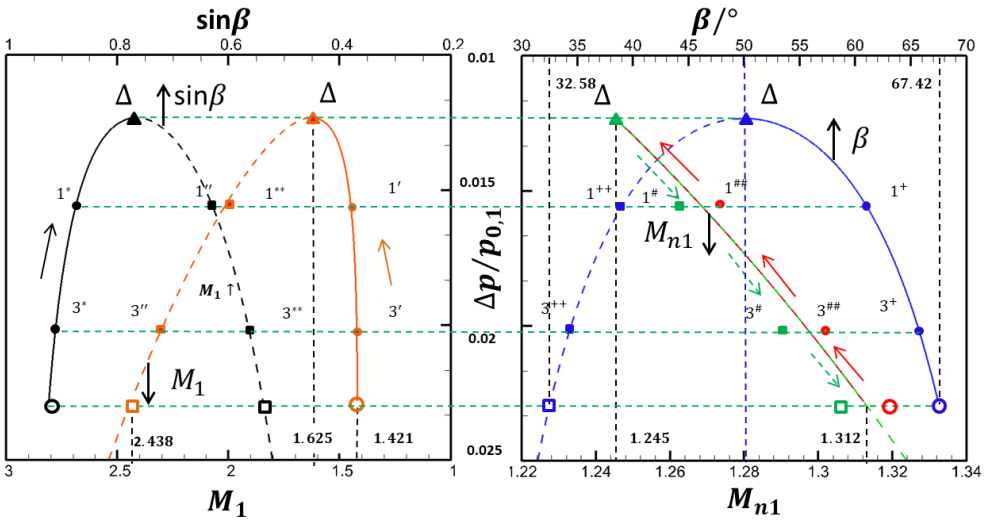

Figure 3 – The two-solutions properties for corresponding β, M_1 at the same M_{n1} (θ=10°).

3. Numerical calculation setting

In order to make the benchmark case modelling, a wedge model in uniform flow is used in figure 4. The supersonic flow through the wedge will generate an oblique shock waves, which can be used to test one new scheme. Avoiding the influence caused by the angle between the mesh and the shock wave, an oblique mesh is adopted in figure 5.

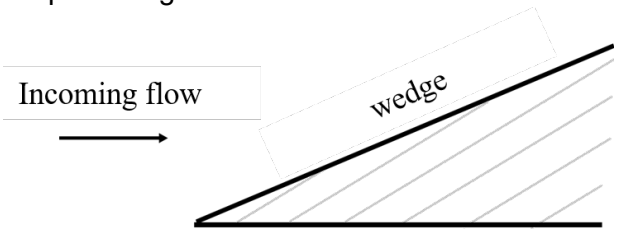

Figure 4 – Wedge model in uniform flow.

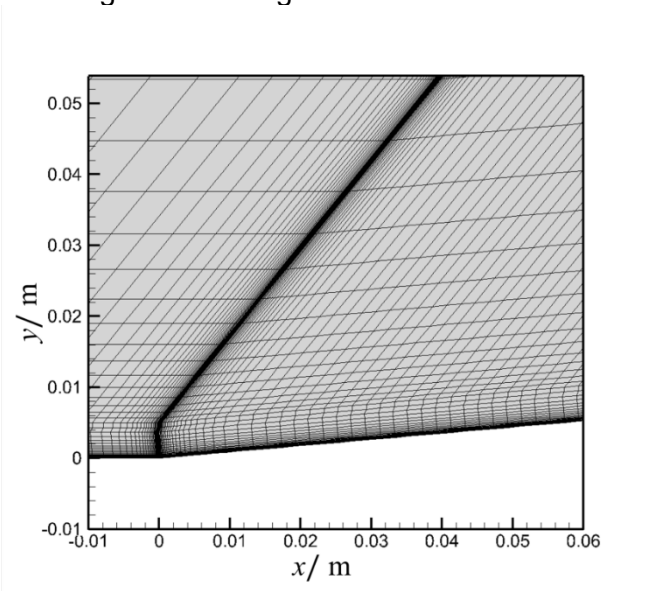

Figure 5 – The oblique mesh of wedge shock numerical simulation.

The finite volume method is used to calculate the flow field. The main calculation programs are Stanford University Unstructured (SU2) and Platform for Hybrid engineering simulation of flows (PHengLEI). Both SU2 and PHengLEI are open source aerodynamic calculation program, which are relatively mature in compressible flow field calculation and aerodynamic optimization. Of course, due to their open source characteristics, various numerical methods can be modified conveniently.

For SU2, six up-wind schemes convection term discrete methods are provided among the numerical methods. They are respectively Roe, HLLC and Cusp, AUSM, AUSM+UP and AUSM+UP2. The highest spatial format is the second order, and the approach of MUSCL (Monotone Upstream - Centered Schemes for Conservation Laws) is adopted. The limiter is Venkatakrishnan type, and the coefficient is 0.005. For PHengLEI, it supports Roe, Van leer, AUSM, steger-warming and so on, which are listed in the table 1.

This paper mainly calculates the physical model with wedge angle of 3, 5 and 7 degrees, the calculation points of Mach number are in 1.1957 ~ 2.3000 with total of 9 state points. The equal shock strength cases are selected on purpose.

Table 1 – The discretization schemes supported by SU2 and PHengLEI

Schemes	Roe	AUSM	AUSMDV	AUSMPW	AUSM+UP	AUSM+UP2	Vanleer	Steger	HLLC	HLLE	CUSP
SU2	✓	✓			✓	✓			✓		✓
PHengLEI	✓		✓	✓			✓	✓		✓	

4. Illustrative results

To measure the accuracy of shock strength capture by various discretization schemes, the ratio of static pressure increment P= (p_2-p_1)/ p_1 is used to describe the shock strength. For an oblique shock wave, the shock strength can be defined as follows.

$$\mathrm{P} = \frac{2\gamma}{\gamma+1}\left(M_{n1}^2 - 1\right) \tag{7}$$

As a basic test example, high-precision experimental results from the Delft University supersonic wind tunnel are applied to check the theoretical model at a deflection angle of three degrees in Figure 6a. Some theoretical benchmark results, CFD computed results and wind tunnel results are compared in Figure 6b. Further studies will cover the other shock strength quantities for the several previously mentioned spatial schemes (ROE, HLLC, AUSM, AUSM+UP, AUSM+UP2 and CUSP) and corresponding adaptive mesh techniques.

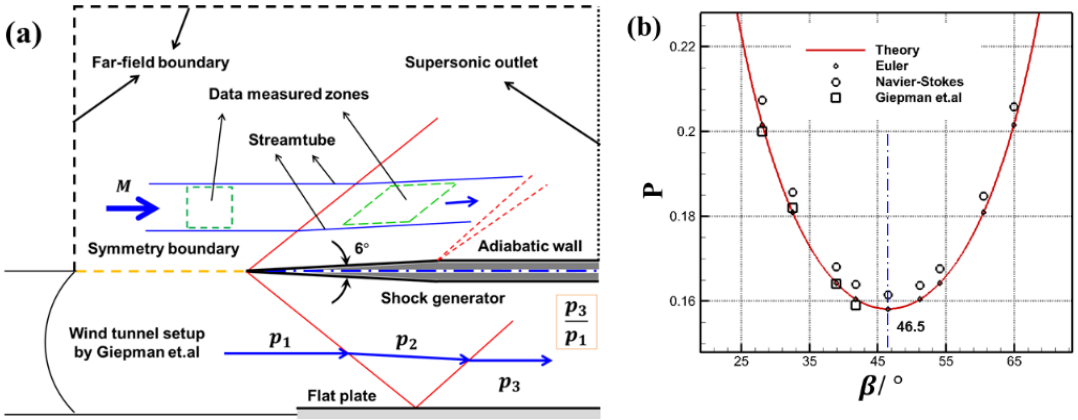

Figure 6 – A comparison of computational and experimental model data for shock intensities from several sources including Euler and NS CFD simulations and experimental results from Delft University.

4.1 Example by SU2

4.1.1 Wedge angle of 3 degrees

It can be seen from figure 6 that the result of Euler equation solution is very close to the theoretical value, indicating that in the inviscid flow, the intensity symmetry of oblique shock wave can be well reflected. However, the intensity of oblique shock wave calculated by N-S equation is larger on the whole, and the experimental value also conforms well to a certain extent.

To obtain the more detailed differences, we calculate a set of result by SU2 focusing on the inviscid flow. As shown in figure 7, it can be seen that the numerical results calculated by SU2 in different discrete schemes are very close to the theoretical Euler results, and the differences between spatial schemes are also very small. In order to better identify the differences, we provide Table 2 and Table 3. The table 2 gives the details of shock strength calculated by different discretization schemes. The table 3 lists the relative errors, in which the number representing the relative errors is ten thousand fractions. Among the nine selected data points, the average relative error of CUSP scheme is the smallest, while the average relative error of HLLC scheme is the largest. The performance of AUSM+UP2 scheme is not as good as AUSM+UP scheme, indicating that the second-order upwind scheme is not better than the first-order upwind scheme in all cases in a way. On the other hand, it also shows that the oblique shock model has ability to distinguish the differences between various discretization schemes.

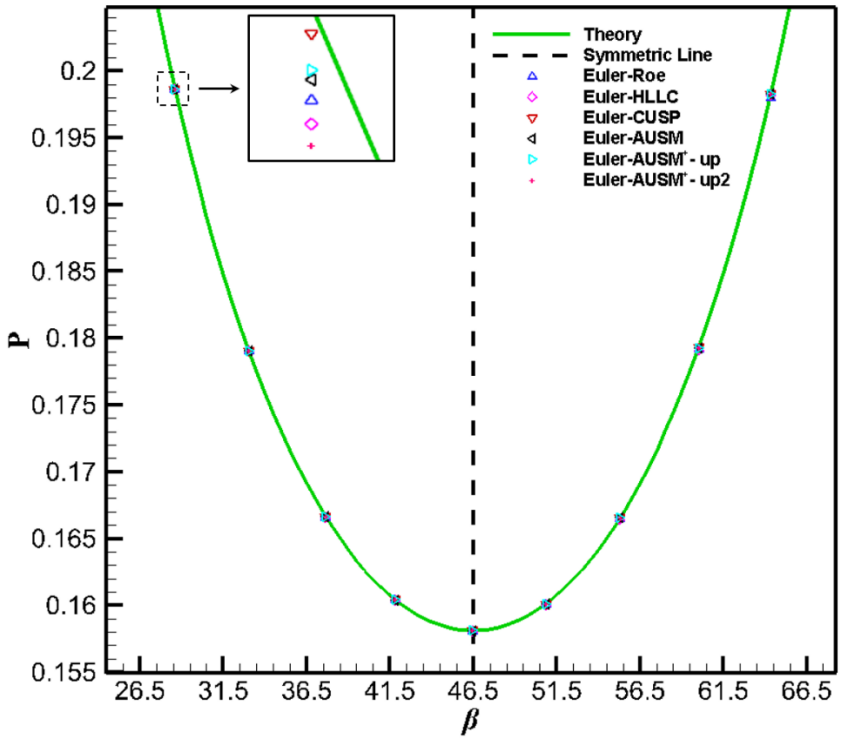

Figure 7 – The result of 3 degrees of deflection angle using six spatial schemes by SU2 program

Table 2 – Theoretical value and shock intensity of 3 degrees of deflection angle calculated by different schemes (SU2)

	P								
	Ma	β	Theory	Roe	HLLC	CUSP	AUSM	AUSM+UP	AUSM+UP2
SU2	1.200	64.34	0.19829	0.19816	0.19819	0.19829	0.19827	0.19829	0.19828
	1.240	60.02	0.17927	0.17919	0.17914	0.17929	0.17923	0.17925	0.17924
	1.300	55.32	0.16657	0.16651	0.16646	0.16657	0.16654	0.16654	0.16653
	1.375	50.86	0.16012	0.16007	0.16004	0.16012	0.16009	0.16011	0.16012
	1.470	46.46	0.15813	0.15809	0.15807	0.15812	0.15809	0.15812	0.15812
	1.600	41.80	0.16045	0.16042	0.16039	0.16043	0.16040	0.16043	0.16042
	1.750	37.65	0.16663	0.16659	0.16659	0.16663	0.16662	0.16662	0.16662
	1.970	33.04	0.17907	0.17905	0.17904	0.17907	0.17905	0.17906	0.17906
	2.260	28.60	0.19863	0.19861	0.19860	0.19863	0.19862	0.19862	0.19859

Table 3 – The relative error of different schemes in 3 degrees of deflection angle (SU2)

	Relative error ‰								
	Ma	β	Theory	Roe	HLLC	CUSP	AUSM	AUSM+UP	AUSM+UP2
SU2	1.200	64.34	0.19829	-6.1641	-4.8346	0.4230	-0.7252	0.4230	-0.3022
	1.240	60.02	0.17927	-4.7362	-7.2359	1.1841	-2.3023	-1.1841	-1.6445
	1.300	55.32	0.16657	-3.5017	-7.0034	0.0000	-2.0800	-2.1710	-2.5212
	1.375	50.86	0.16012	-3.2604	-5.0717	-0.0362	-2.2098	-0.7970	-0.3623
	1.470	46.46	0.15813	-2.5634	-3.7353	-0.1465	-2.1972	-0.5859	-0.6592
	1.600	41.80	0.16045	-1.8443	-3.2547	-0.7956	-2.7484	-0.8679	-1.8805
	1.750	37.65	0.16663	-2.7305	-2.8005	-0.3501	-0.7701	-0.8401	-0.7001
	1.970	33.04	0.17907	-1.1852	-2.1070	0.0000	-1.3169	-0.6584	-0.9876
	2.260	28.60	0.19863	-1.0862	-1.5086	0.0000	-0.7241	-0.6034	-1.8405
		Average		-3.0080	-4.1724	0.0310	-1.6749	-0.8094	-1.2109

4.1.2 Wedge angle of 5 degrees

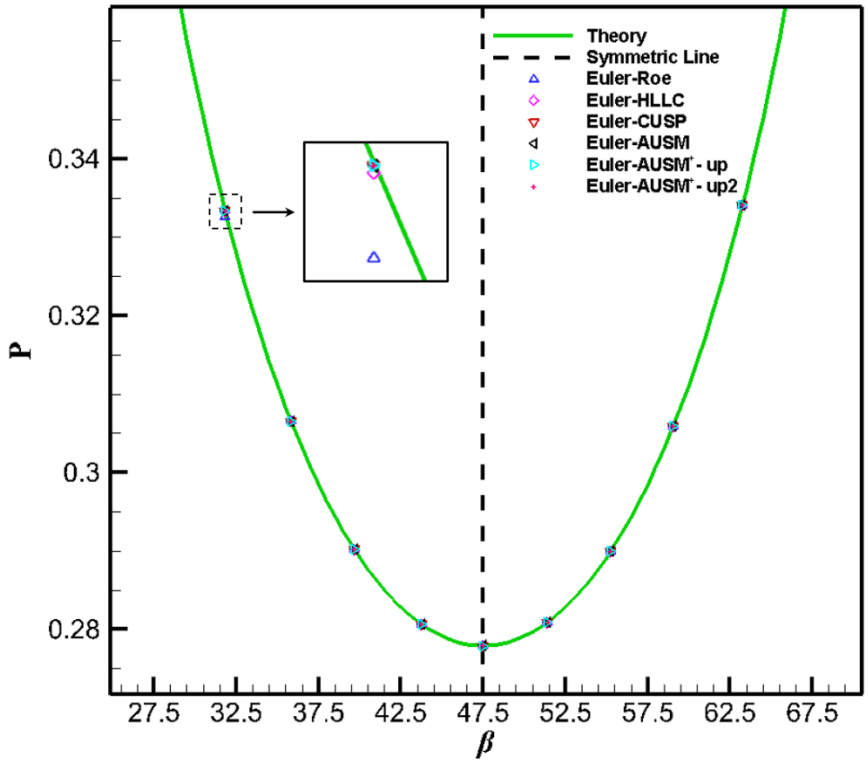

Figure 8 – The result of 5 degrees using six spatial schemes by SU2 program

Table 4 – Theoretical value and shock intensity of 5 degrees of deflection angle calculated by different schemes (SU2)

			P						
	Ma	β	Theory	Roe	HLLC	CUSP	AUSM	AUSM+UP	AUSM+UP2
SU2	1.270	63.26	0.33407	0.33379	0.33300	0.33406	0.33391	0.33403	0.33411
	1.310	59.05	0.30588	0.30563	0.30539	0.30587	0.30575	0.30587	0.30588
	1.360	55.25	0.28995	0.28973	0.28957	0.28995	0.28983	0.28993	0.28995
	1.425	51.42	0.28093	0.28070	0.28066	0.28093	0.28084	0.28092	0.28092
	1.510	47.47	0.27795	0.27777	0.27770	0.27794	0.27786	0.27786	0.27793
	1.610	43.77	0.28065	0.28048	0.28040	0.28062	0.28052	0.28061	0.28062
	1.750	39.68	0.29018	0.29003	0.28998	0.29016	0.29010	0.29018	0.29018
	1.920	35.82	0.30656	0.30643	0.30636	0.30663	0.30656	0.30656	0.30656
	2.150	31.83	0.33335	0.33324	0.33319	0.33259	0.33328	0.33334	0.33334

Table 5 – The relative error of different schemes in 5 degrees of deflection angle (SU2)

	Relative error ‰								
	Ma	β	Theory	Roe	HLLC	CUSP	AUSM	AUSM+UP	AUSM+UP2
SU2	1.270	63.26	0.33407	-8.3861	-31.9472	-0.3993	-4.7921	-1.1980	1.1980
	1.310	59.05	0.30588	-8.1116	-16.2231	-0.2135	-4.2692	-0.4269	0.0427
	1.360	55.25	0.28995	-7.5631	-12.9018	-0.0445	-4.0485	-0.4449	0.0000
	1.425	51.42	0.28093	-8.2073	-9.5751	-0.2280	-3.1917	-0.4560	-0.4560
	1.510	47.47	0.27795	-6.4369	-9.1955	-0.4598	-3.4483	-3.2184	-0.6897
	1.610	43.77	0.28065	-5.9321	-8.6700	-0.9126	-4.5632	-1.3690	-1.1408
	1.750	39.68	0.29018	-4.8908	-6.6693	-0.4446	-2.6677	-0.0445	0.0445
	1.920	35.82	0.30656	-4.2620	-6.3930	2.1310	0.0426	-0.0426	0.0000
	2.150	31.83	0.33335	-3.1999	-4.7998	-22.7991	-1.9999	-0.2000	-0.4000
		Average		-6.3322	-11.8194	-2.5967	-3.2153	-0.8222	-0.1557

4.1.3 Wedge angle of 7 degrees

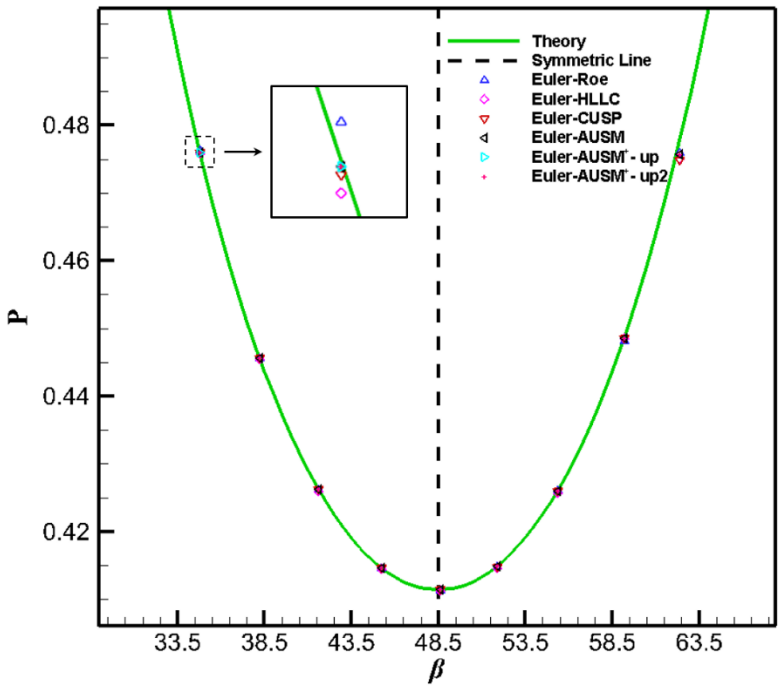

Figure 9 – The result of 7 degrees using six spatial schemes by SU2 program

Table 6 – Theoretical value and shock intensity of 7 degrees of deflection angle calculated by different schemes (SU2)

			P						
	Ma	β	Theory	Roe	HLLC	CUSP	AUSM	AUSM+UP	AUSM+UP2
SU2	1.340	62.37	0.47758	0.47377	0.47049	0.47596	0.47507	0.47478	0.47566
	1.370	59.19	0.44868	0.44752	0.44563	0.44810	0.44853	0.44853	0.44853
	1.420	55.37	0.42614	0.42557	0.42498	0.42614	0.42571	0.42600	0.42600
	1.480	51.88	0.41490	0.41434	0.41404	0.41483	0.41461	0.41479	0.41493
	1.550	48.62	0.41144	0.41101	0.41080	0.41137	0.41132	0.41141	0.41145
	1.640	45.23	0.41469	0.41429	0.41413	0.41468	0.41444	0.41468	0.41469
	1.760	41.60	0.42627	0.42584	0.42577	0.42624	0.42599	0.42627	0.42627
	1.900	38.22	0.44564	0.44529	0.44520	0.44559	0.44546	0.44564	0.44564
	2.080	34.78	0.47597	0.47564	0.47566	0.47629	0.47582	0.47594	0.47600

Table 7 – The relative error of different schemes in 7 degrees of deflection angle (SU2)

			Relative error ‰						
	Ma	β	Theory	Roe	HLLC	CUSP	AUSM	AUSM+UP	AUSM+UP2
SU2	1.340	62.37	0.47758	-79.8219	-148.5059	-34.0326	-52.5958	-58.7836	-40.2203
	1.370	59.19	0.44868	-25.8302	-67.8044	-12.9151	-3.2288	-3.2288	-3.2288
	1.420	55.37	0.42614	-13.3866	-27.1079	0.0000	-10.0400	-3.3467	-3.3467
	1.480	51.88	0.41490	-13.6408	-20.8023	-1.7051	-7.1614	-2.7282	0.6820
	1.550	48.62	0.41144	-10.2915	-15.4373	-1.7153	-2.7444	-0.6861	0.3431
	1.640	45.23	0.41469	-9.5520	-13.6457	-0.3411	-6.1406	-0.3411	0.0000
	1.760	41.60	0.42627	-10.0378	-11.7107	-0.6692	-6.6919	0.0000	0.0000
	1.900	38.22	0.44564	-7.7856	-9.7320	-0.9732	-3.8928	0.0000	0.0000
	2.080	34.78	0.47597	-6.8222	-6.5121	6.8222	-3.1010	-0.6202	0.6202
		Average		-19.6854	-35.6954	-5.0588	-10.6218	-7.7483	-5.0167

4.1.4 Wedge angle of 10 degrees

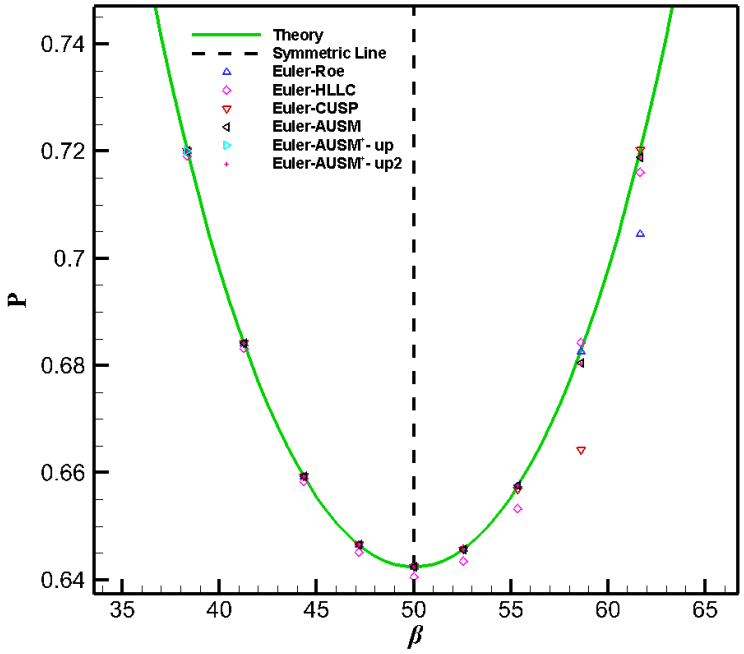

Figure 10 – The result of 10 degrees using six spatial schemes by SU2 program

Table 8 – Theoretical value and shock intensity of 10 deflection angle calculated by different schemes (SU2)

			P						
	Ma	β	Theory	Roe	HLLC	CUSP	AUSM	AUSM+UP	AUSM+UP2
SU2	1.445	61.64	0.71987	0.71815	0.71677	0.70456	0.71609	0.72021	0.71884
	1.475	58.61	0.68276	0.68243	0.68646	0.68259	0.68428	0.66425	0.68041
	1.520	55.35	0.65749	0.64904	0.64887	0.65741	0.65335	0.65683	0.65766
	1.570	52.55	0.64576	0.64214	0.64066	0.64574	0.64345	0.64568	0.64573
	1.625	50.02	0.64238	0.63992	0.63893	0.64240	0.64066	0.64237	0.64238
	1.700	47.17	0.64656	0.64499	0.64409	0.64656	0.64524	0.64656	0.64656
	1.790	44.34	0.65933	0.65800	0.65733	0.65931	0.65833	0.65933	0.65933
	1.910	41.26	0.68415	0.68280	0.68247	0.68413	0.68331	0.68413	0.68413
	2.050	38.34	0.72009	0.71888	0.71880	0.72009	0.71906	0.72009	0.72009

Table 9 – The relative error of different schemes in 10 deflection angle (SU2)

	Relative error ‰								
	Ma	β	Theory	Roe	HLLC	CUSP	AUSM	AUSM+UP	AUSM+UP2
SU2	1.445	61.64	0.71987	-23.8914	-43.0046	-212.6336	-52.5611	4.7783	-14.3349
	1.475	58.61	0.68276	-4.9293	54.2220	-2.4646	22.1817	-271.1102	-34.5049
	1.520	55.35	0.65749	-128.5676	-131.0885	-1.2605	-63.0233	-10.0837	2.5209
	1.570	52.55	0.64576	-56.0685	-79.0056	-0.2549	-35.6799	-1.2743	-0.5097
	1.625	50.02	0.64238	-38.3505	-53.6908	0.2557	-26.8454	-0.2557	0.0000
	1.700	47.17	0.64656	-24.1932	-38.1998	0.0000	-20.3732	0.0000	0.0000
	1.790	44.34	0.65933	-20.1336	-30.2004	-0.2517	-15.1002	0.0000	0.0000
	1.910	41.26	0.68415	-19.6933	-24.6167	-0.2462	-12.3083	-0.2462	-0.2462
	2.050	38.34	0.72009	-16.7210	-17.9154	0.0000	-14.3323	0.0000	0.0000
		Average		-36.9498	-40.3888	-24.0951	-24.2269	-30.9102	-5.2305

In order to make the result more convincing, the CFD results of wedge of 5, 7 and 10 degrees are supplemented, as shown in table 4 to 9 and figure 8, 9, 10. With the increase of wedge Angle, the absolute value of the relative error tends to increase, such as the absolute value of relative error of Roe scheme is increasing from 3.0080‰ to 36.9498‰. The differences between the various schemes are also amplified, which is beneficial for verifying a new scheme. The calculation results of different schemes at different deflection angles cannot always maintain the best effect. For deflection angle of 3 degrees, the CUSP scheme has the smallest relative error, however for deflection angle of 5 degrees, the AUSM+UP2 scheme is the smallest. That is to say, discretization schemes would have their own ranges of applicability, some have the better efficiency for small disturbance, others for bigger deflection angle.

The level of disturbance can also affect the performance of various discretization schemes in CFD process. When the disturbance reaches a certain degree, some discretization schemes start to become sensitive, and a small change in wedge angle may lead to a large change in the calculated relative error.

An interesting phenomenon should be mentioned. In the case of equal shock intensity, the relative errors calculated by various discretization schemes at large shock angle and small Mach number are generally larger than those calculated at small shock angle and large Mach number. This is especially obvious at large deflection angle.

4.2 Example by PHengLEI

PHengLEI is a structural/unstructural general purpose CFD open source program, whose calculation range covers low speed, subsonic, transonic and hypersonic. More importantly, this program also supports higher-precision schemes such as Weight compact nolinear scheme (WCNS). This section will show the CFD results of the wedge of three degrees, including the shock strength and entropy, which is supplemented and compared with the results of SU2.

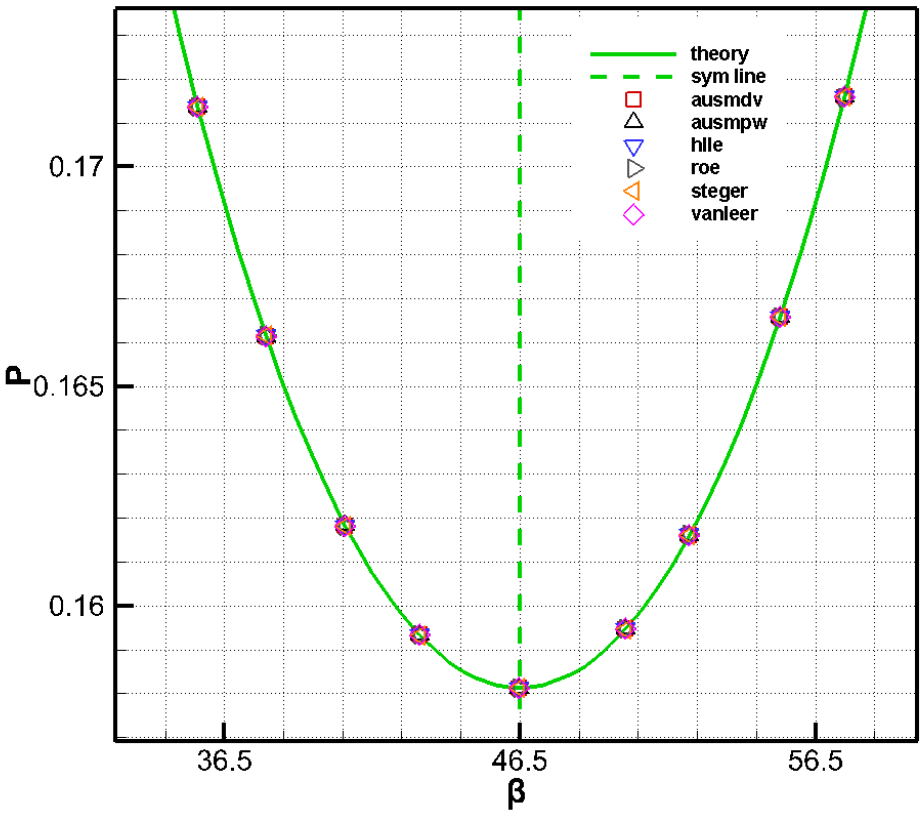

Figure 11 – The result of 3 degrees using six spatial schemes by PHengLEI program

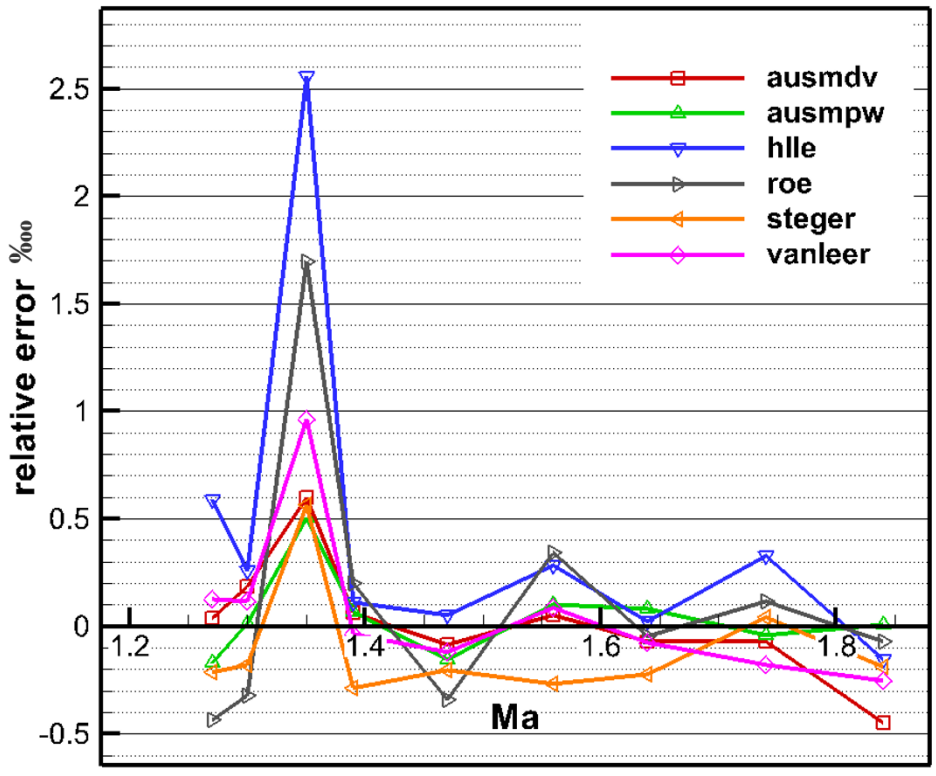

Figure 12 – The relative errors (ten thousandth) of shock intensity calculated by the six discretization schemes at different incoming Mach numbers when wedge angle is three degrees

Table 10 – Theoretical value and shock intensity of 3 degrees of deflection angle calculated by different schemes (PHengLEI)

			P						
	Ma	β	Theory	Roe	HLLE	Steger	Vanleer	AUSMPW	AUSMDV
PHengLEI	1.27	57.49245015	0.17159084	0.17158336	0.17160098	0.17158720	0.17159300	0.17158792	0.17159148
	1.30	55.31703782	0.16657265	0.16656731	0.16657694	0.16656967	0.16657462	0.16657285	0.16657573
	1.35	52.22070239	0.16159083	0.16161823	0.16163213	0.16159991	0.16160636	0.16159900	0.16160050
	1.39	50.08701857	0.15947384	0.15947705	0.15947561	0.15946926	0.15947326	0.15947489	0.15947481
	1.47	46.46125986	0.15812680	0.15812138	0.15812763	0.15812354	0.15812490	0.15812440	0.15812545
	1.56	43.10967374	0.15932922	0.15933465	0.15933378	0.15932496	0.15933057	0.15933086	0.15933006
	1.64	40.59232008	0.16182645	0.16182570	0.16182685	0.16182285	0.16182519	0.16182778	0.16182531
	1.74	37.89916418	0.16614601	0.16614793	0.16615145	0.16614673	0.16614304	0.16614531	0.16614480
	1.84	35.59316223	0.17136719	0.17136597	0.17136454	0.17136398	0.17136286	0.17136732	0.17135946

Table 11 – The relative error of shock intensity calculated by different schemes in 3 deflection angle (PHengLEI)

			Relative error ‰						
	Ma	β	Theory	Roe	HLLE	Steger	Vanleer	AUSMPW	AUSMDV
PHengLEI	1.27	57.49245015	0.17159084	-0.43625422	0.59085087	-0.21228180	0.12544835	-0.17014299	0.03681082
	1.30	55.31703782	0.16657265	-0.32069382	0.25750786	-0.17902832	0.11862031	0.01189029	0.18515510
	1.35	52.22070239	0.16159083	1.69581087	2.55600293	0.56188030	0.96111797	0.50548082	0.59839756
	1.39	50.08701857	0.15947384	0.20152656	0.11143219	-0.28720314	-0.03597349	0.06628027	0.06094625
	1.47	46.46125986	0.15812680	-0.34264428	0.05219093	-0.20591653	-0.11996521	-0.15204216	-0.08550585
	1.56	43.10967374	0.15932922	0.34065964	0.28603190	-0.26782812	0.08450759	0.10254363	0.05234017
	1.64	40.59232008	0.16182645	-0.04619590	0.02488088	-0.22242541	-0.07800610	0.08249165	-0.07012045
	1.74	37.89916418	0.16614601	0.11579581	0.32769782	0.04357711	-0.17847785	-0.04179342	-0.07237154
	1.84	35.59316223	0.17136719	-0.07074481	-0.15466766	-0.18733290	-0.25253962	0.00757433	-0.45100104
	Average			0.12636221	0.45021419	-0.10628431	0.06941466	0.04580916	0.02829456

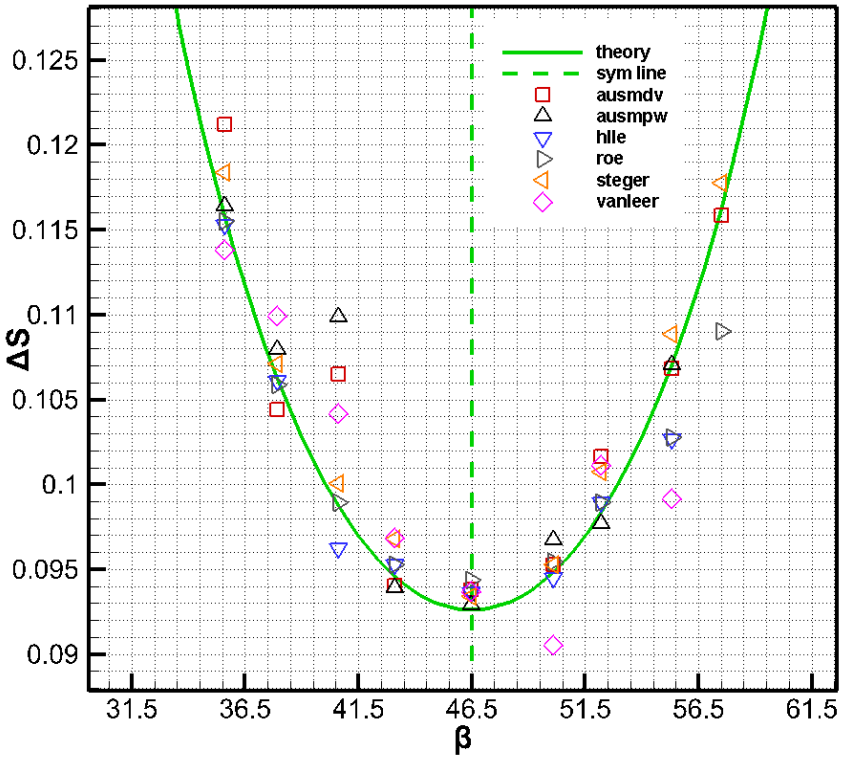

Figure 13 – The entropy production across the shock wave calculated by the six discretization schemes when wedge angle is three degrees

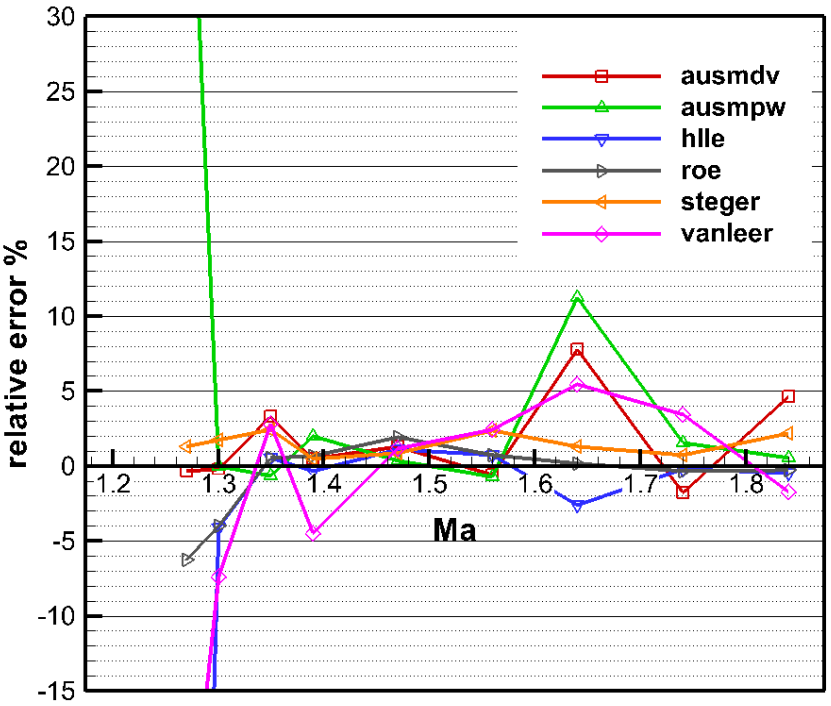

Figure 14 – The relative errors (percentage) of entropy production calculated by the six discretization schemes at different incoming Mach numbers when wedge angle is three degrees

Table 12 – Theoretical value and entropy production of 3 degrees of deflection angle calculated by different schemes (PHengLEI)

	ΔS								
	Ma	β	Theory	Roe	HLLE	Steger	Vanleer	AUSMPW	AUSMDV
PHengLEI	1.27	57.49245015	0.11624039	0.10901020	0.01679061	0.11776439	0.08368625	0.17378378	0.11584183
	1.30	55.31703782	0.10704553	0.10278184	0.10266107	0.10888656	0.09915695	0.10705987	0.10684813
	1.35	52.22070239	0.09837379	0.09892433	0.09892015	0.10074301	0.10115501	0.09772393	0.10166621
	1.39	50.08701857	0.09482458	0.09545968	0.09451653	0.09528722	0.09056462	0.09672228	0.09528827
	1.47	46.46125986	0.09260798	0.09438556	0.09363468	0.09339983	0.09372644	0.09291448	0.09381677
	1.56	43.10967374	0.09458506	0.09528086	0.09529192	0.09680905	0.09686661	0.09391734	0.09403812
	1.64	40.59232008	0.09877379	0.09891794	0.09623670	0.10006104	0.10417149	0.10989199	0.10648983
	1.74	37.89916418	0.10628519	0.10590270	0.10608157	0.10708969	0.10992747	0.10796919	0.10439944
	1.84	35.59316223	0.11582064	0.11551090	0.11528174	0.11837471	0.11383709	0.11642210	0.12122410

Table 13 – The relative error of entropy production calculated by different schemes in 3 deflection angle (PHengLEI)

	Relative error %								
	Ma	β	Theory	Roe	HLLE	Steger	Vanleer	AUSMPW	AUSMDV
PHengLEI	1.27	57.49245015	0.17159084	-6.22002842	-85.55526951	1.31108142	-28.00587737	49.50378580	-0.34287320
	1.30	55.31703782	0.16657265	-3.98306433	-4.09588024	1.71985872	-7.36936706	0.01339492	-0.18440736
	1.35	52.22070239	0.16159083	0.55964887	0.55539701	2.40839306	2.82719734	-0.66059890	3.34685205
	1.39	50.08701857	0.15947384	0.66976127	-0.32486163	0.48789289	-4.49246769	2.00127752	0.48899255
	1.47	46.46125986	0.15812680	1.91946719	1.10865453	0.85505122	1.20773880	0.33096399	1.30527573
	1.56	43.10967374	0.15932922	0.73563129	0.74732402	2.35131015	2.41216819	-0.70595193	-0.57825509
	1.64	40.59232008	0.16182645	0.14594399	-2.56858456	1.30322885	5.46471148	11.25622837	7.81182824
	1.74	37.89916418	0.16614601	-0.35986689	-0.19157586	0.75692815	3.42689728	1.58442348	-1.77423136
	1.84	35.59316223	0.17136719	-0.26743336	-0.46529144	2.20518660	-1.71260711	0.51929507	4.66536828
		Average		-0.75554893	-10.08778752	1.48877012	-2.91573402	7.09364648	1.63761665

Similarly, to SU2, the difference between the calculated shock wave intensity and the theoretical value is very small under the six schemes, which are all less than 0.026%. It cannot tell the differences via figure 11. According to figure 12, we can find that differences do exist between the different schemes. Compared with other schemes, the average error of HLLE scheme is the largest. Overall, AUSMDV scheme had the best effect, with an average relative error of only 0.00028%. Another interesting phenomenon is that, in the trend, the relative errors of the six schemes all reach the peak at Mach number 1.35. Perhaps there is some incentive at this Mach number that leads to the maximum errors of the six schemes at the same time. One can get more information from table 10 and 11.

Be different from the ratio of static pressure increment P, the entropy increase across shock wave has obvious difference in figure 13. It presents a state of incomplete uneven. The relative error also becomes more diacritical (figure 14), which proves that entropy increase can be a good metric for measuring discrete one new scheme. More details of data are provided in table 12 and 13.

Acknowledgements

The authors gratefully acknowledge China Aerodynamics Research and Development Center - CARDC providing the open-source CFD code of PHengLei in version 7268.

Copyright Statement

The authors confirm that they, and/or their company or organization, hold copyright on all of the original material included in this paper. The authors also confirm that they have obtained permission, from the copyright holder of any third party material included in this paper, to publish it as part of their paper. The authors confirm that they give permission, or have obtained permission from the copyright holder of this paper, for the publication and distribution of this paper as part of the ICAS proceedings or as individual off-prints from the proceedings.

References

[1] Anderson, J. D., Fundamentals of Aerodynamics, 6th ed. The McGraw-Hill Companies Inc, 2017.

[2] Giepman, R., Schrijer, F., & Van Oudheusden, B. A parametric study of laminar and transitional oblique shock wave reflections. J. Fluid Mech. 2018, 844, 187-215.

[3] Shi, A M, Dowell, E H. Theoretical solutions and physical significances for minimum ratio of total pressure loss by oblique shock [J]. Acta Aeronautica et Astronautica Sinica, 2018, 39(12): 122517.